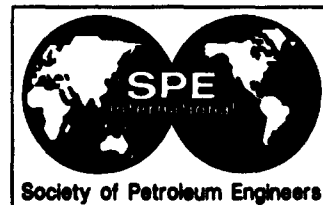


**SPE 29111**



## **Compositional and Black Oil Reservoir Simulation**

K.H. Coats, K.H. Coats and Company Inc., L.K. Thomas, and R.G. Pierson, Phillips Petroleum Company

SPE Members

Copyright 1995, Society of Petroleum Engineers, Inc.

This paper was prepared for presentation at the 13th SPE Symposium on Reservoir Simulation held in San Antonio, TX, U.S.A., 12-15 February 1995.

This paper was selected for presentation by an SPE Program Committee following review of information contained in an abstract submitted by the author(s). Contents of the paper, as presented, have not been reviewed by the Society of Petroleum Engineers and are subject to correction by the author(s). The material, as presented, does not necessarily reflect any position of the Society of Petroleum Engineers, its officers, or members. Papers presented at SPE meetings are subject to publication review by Editorial Committees of the Society of Petroleum Engineers. Permission to copy is restricted to an abstract of not more than 300 words. Illustrations may not be copied. The abstract should contain conspicuous acknowledgment of where and by whom the paper is presented. Write Librarian, SPE, P.O. Box 833836, Richardson, TX 75083-3836, U.S.A. Telex, 163245 SPEUT.

### **Abstract**

This paper describes a three-dimensional, three-phase reservoir simulation model for black oil and compositional applications. Both IMPES and fully implicit formulations are included. The model's use of a relaxed volume balance concept effectively conserves both mass and volume and reduces Newton iterations. A new implicit well rate calculation method improves IMPES stability. It approximates wellbore crossflow effects with high efficiency and relative simplicity in both IMPES and fully implicit formulations. Multiphase flow in the tubing and near-well turbulent gas flow effects are treated implicitly.

Initial saturations are calculated as a function of water-oil and gas-oil capillary pressures which are optionally dependent upon the Leverett J function or initial saturations may be entered as data arrays. A normalization of the relative permeability and capillary pressure curves is used to calculate these terms as a function of rock type and grid block residual saturations.

Example problems are presented, including several of the SPE Comparative Solution problems and field simulations.

### **Introduction**

This paper describes a numerical model for simulating three-dimensional, three-phase flow in heterogeneous, single-

porosity reservoirs. The model, which is referred to as Sensor, incorporates black oil and fully compositional capabilities formulated in both IMPES and fully implicit modes. The formulations include a relaxed volume concept and a new method for implicit treatment of well rates with wellbore crossflow. Following model description, several example problems are presented. They include five SPE Comparative Solution Project problems, a turbulent gas flow problem, a crossflow problem, and three field studies.

### **General Description of the Model**

The model simulates three-dimensional, three-phase flow in heterogeneous, single-porosity porous media. The usual viscous, gravity and capillary forces are represented by Darcy's law modified for relative permeability. The flow is isothermal although, as an option, a spatially variable, time invariant temperature distribution may be specified in the compositional case.

The conventional seven-point orthogonal Cartesian  $xyz$  grid and the cylindrical  $r-\theta-z$  grid are used. Mapping or linear indexing is used to require storage and arithmetic only for active grid blocks.

The model includes both black oil and fully compositional capabilities. The black oil option includes the  $r$ , stb/scf term as well as the normal  $R$ , solution gas term. It therefore applies to gas condensate and black oil problems. Interfacial tension, modifying gas-oil capillary pressure, is also entered versus pressure in the black oil PVT table. The compositional case

---

References and illustrations at end of paper

utilizes the Peng Robinson (PR)<sup>1</sup> or Soave Redlich Kwong (SRK)<sup>2</sup> equation of state. Shift factors<sup>3</sup> are included to account for volume translation<sup>4</sup>. The compositional case optionally uses tabular K-values versus  $p$ , rather than equation of state fugacity-based K-values. The table is generated internally by an expansion of the original reservoir fluid. This option applies near-rigorously to cases of natural depletion with or without water injection and/or influx. It is significantly more efficient than use of the equation of state in the IMPES case.

The effect of pore collapse and compaction is incorporated in the model using the logic presented by Sulak et al<sup>5</sup>. Hysteresis of rock compressibility is included in the calculation to account for the irreversible effect of pore collapse. Two-dimensional compaction tables relate rock compressibility to porosity and stress. Each grid block is then assigned to one of these tables. If no tables are entered, then porosity is  $\phi_b (1 + c_r (p-p_b))$  where  $\phi_b$  is entered for each grid block.

IMPES and fully implicit (FI) formulations are coded for both the black oil and compositional cases. The linear solvers include direct D4<sup>6</sup>, block SOR<sup>7</sup>, and a conjugate gradient solver<sup>8,9</sup>. The SOR uses either  $xz$  or  $yz$  planes as blocks and optionally incorporates Watts correction<sup>10</sup>. Well rate terms including wellbore crossflow are implicit in both formulations. The wellbore constraint equations<sup>11,12</sup> are also fully implicit to achieve "exact" target rates even in the IMPES case.

**Mathematical Description of the Model**

The model consists of  $N = 2N_c + 4$  equations for each active grid block and  $N_w$  well constraint equations for active wells which are not on pressure constraint. The  $N$  equations include mass balances for  $N_c$  hydrocarbon components and water:

$$\frac{V}{\Delta t} \delta [(\rho_o S_o x_i + \rho_g S_g y_i)] - \Delta \left[ T \rho_o x_i \frac{k_{ro}}{\mu_o} (\Delta p - \Delta P_{cgo} - \gamma_o \Delta Z) \right] + \Delta \left[ T \rho_g y_i \frac{k_{rg}}{\mu_g} (\Delta p - \gamma_g \Delta Z) \right] - q_i, \dots \dots \dots (1a)$$

$i = 1, 2, \dots, N_c$

$$\frac{V}{\Delta t} \delta (\phi b_w S_w) = \Delta [T b_w \frac{k_{rw}}{\mu_w} (\Delta p - \Delta P_{cgo} - \Delta P_{cwo} - \gamma_w \Delta Z)] - q_w \dots \dots \dots (1b)$$

In addition to these  $N_c + 1$  equations, there are  $N_c + 3$  constraint equations for each grid block:  $N_c$  phase equilibrium constraints, and the summations to 1.0 of  $y_i, x_i,$  and  $S_w, S_o, S_g$ .

It is well known that a black oil PVT table including formation volume factors,  $R_s$  and  $r_s$  versus pressure can be converted to compositional mode. The converted table gives the saturated oil and gas phase molar densities (moles/rb) and compositions (mole

fractions  $x_i$  and  $y_i$ ) as single-valued functions of pressure. Thus, equations 1 and the constraints apply unchanged to the black oil case. Only the implicit and IMPES formulations require description, with appropriate comment regarding compositional equation of state PVT versus the simpler black oil PVT.

The model formulation is an alteration of one previously described<sup>13</sup>. That paper's linearization renders the model equations for a grid block in the single matrix equation form,

$$C \delta P = \Delta(T \Delta \delta P) + R \dots \dots \dots (2)$$

Transmissibility  $T$  and  $C$  are  $N_c + 1 \times N_c + 1$  matrices and unknown  $P$  and residual  $R$  are  $N_c + 1$  column vectors. The  $T$  matrix elements are calculated using upstream phase mobilities, densities, and compositions. In the IMPES case  $T$  is empty but for column  $N_c + 1$ . That column,  $T_{N_c + 1}$ , contains the pressure transmissibilities, calculated using explicit phase mobilities, densities, and compositions.

The  $N$  variables selected in this linearization process are the natural ones  $\bar{P} = y_i, x_i, S_w, S_o, S_g, p$ . This selection leads to simplicity in constraint expressions and no need for pivoting in Gaussian eliminations. Many authors propose a variety of other variable choices<sup>14,15,16</sup>.

Any term  $X$  in equation 1 has the general form of a product  $X = abc$  and its value at time level  $n + 1$  is approximated by the linearizations using latest iterate  $l$  information.

$$X_{n+1} = X^{l+1} = X^l + \delta X$$

$$\delta X = bc \delta a + ac \delta b + ab \delta c \dots \dots \dots (3)$$

$$\delta a = \sum_{m=1}^N \left[ \frac{\partial a}{\partial P_m} \delta P_m \right]$$

For a three-phase block, the constraints are a set of  $N_c + 3$  equations in the  $N$  variables. Gaussian elimination on them gives an elimination matrix  $E$  relating the  $N_c + 3$  eliminated variables to the  $N_c + 1$  retained or primary variables  $P$  of equation 2,

$$\delta P_c = E \delta P \dots \dots \dots (4)$$

The  $N_c + 3$  variables  $\delta P_c$  are eliminated from the linearized form of equation 1 using this matrix  $E$ .  $E$  is ostensibly an  $N_c + 3 \times N_c + 1$  matrix. Actually it is an  $N_c \times N_c + 1$  matrix due to the simplicity of the three constraints

$$\delta x_{N_c} = - \delta x_1 - \delta x_2 - \dots - \delta x_{N_c-1} \dots \dots \dots (5a)$$

$$\delta y_{N_c} = - \delta y_1 - \delta y_2 - \dots - \delta y_{N_c-1} \dots \dots \dots (5b)$$

$$\delta S_w = \alpha - \delta S_o - \delta S_g \dots \dots \dots (5c)$$

where  $\alpha$  is discussed below. The  $N_c$  eliminated variables in  $P_c$  are  $y_1, y_2, \dots, y_{N_c-1}, x_1$ .  $E$  is formed at the beginning of each

Newton iteration for each three-phase block and stored. The eliminated variables are then calculated from equations 4 and 5 after  $P$  is available from the linear solver's solution of equation 2.

For a three-phase block, the resulting set of  $N_c+1$  primary variables is  $x_2, x_3, \dots, x_{N_c-1}, S_o, S_g, p$ . The primary variables are  $x_1, x_2, \dots, x_{N_c-1}, S_o, p$  for a water-oil block and  $y_1, y_2, \dots, y_{N_c-1}, S_g, p$  for a gas-water block.

The units of each term in equation 2 are moles/d (stb/d for the last, water equation). For an all-water block,  $C$  is a diagonal matrix. For  $i=1, N_c, c_{ii} = 1/\Delta t, c_{N_c+1, N_c+1} = \partial \phi_{b_w} / \partial p \ V / \Delta t$ . If hydrocarbons invade the block, then the values of  $P_i, i=1, N_c$  are directly the number of moles of component  $i$  in the block. Thus, the mass, composition, density and saturation of the hydrocarbon phase(s) can be computed and the block is switched to the appropriate hydrocarbon-water case.

A significant difference from the above formulation is a relaxed volume concept mentioned by several authors in connection with IMPES. IMPES is an implicit pressure, explicit saturation method independently conceived by Stone and Garder<sup>17</sup> and Sheldon et al<sup>18</sup>. Their method is widely used in black oil simulation, generally incorporating the saturation constraint  $S_w + S_o + S_g = 1$ . However, early papers by Wattenbarger<sup>19,20</sup> and Abel et al<sup>21</sup> described IMPES in the compositional and black oil cases with exact mass balance and a relaxed volume balance. Young and Stephenson<sup>14</sup> and others<sup>15,16</sup> more explicitly described the exact mass balances attained by relaxing the volume balance.

We use this concept in both the IMPES and implicit formulations. The saturation constraint is written as equation 5c where  $\alpha$  is  $1 - (S_w + S_o + S_g)^l$ . For both IMPES and implicit cases, the calculation procedure begins as follows.  $E$  and the coefficients for all terms  $C, T$ , and  $R$  of equation 2 are calculated at iteration  $l$ . In the implicit case, equation 2 and the well constraints are then solved by the linear solver. The solution vector  $P$  is (only) used to calculate well rate and interblock flow terms at the  $l+1$  iterate level. The mass of each component in the grid block at iterate  $l+1$  is then calculated as the mass at time level  $n$  plus the net interblock inflow minus the production. The composition and density of each phase are then calculated, using only the pressure component of the solution vector  $P$ .  $S_w$  is calculated as the mass of water present divided by  $l+1$  level water density and pore volume. For a three-phase block, the total hydrocarbon moles are flashed to obtain moles of gas and oil and the phase densities. The oil and gas volumes are calculated as their

mass/density and their saturations as volumes divided by  $l+1$  level pore volume. Thus the three saturations do not add to unity and  $\alpha$  is not zero. But mass balance is exact for all components.

In effect, this procedure amounts to iterating out volume balance rather than mass balance. This introduces another (volume) balance to monitor and report with attendant closure tolerance considerations. The model here allows conventional 1.0 volume balance as an option. In all problems to date we have found this concept an improvement with results showing near-exact volume balance in addition to exact mass balance. Iterations and cpu time are somewhat to significantly less and answers are the same as compared with the conventional 1.0 volume balance approach.

In the IMPES case, the pressure transmissibilities  $T_{N_c+1}$  are not necessarily constant over the time step. If more than one Newton iteration is performed, they are recalculated to account for possible changes in flow direction. They can optionally be left unchanged. The IMPES pressure equation is obtained in a straightforward manner<sup>22</sup>, using the obvious extension of the original black oil IMPES reduction. The  $i^{th}$  equation of the  $N_c+1$  scalar equations comprising equation 2 is multiplied by a factor  $v_i$ , with  $v_{N_c+1} = 1$ , and the resulting  $N_c+1$  equations (rows) are added. The values of  $v_i$  are determined so that this addition reduces the left-hand side to a single term  $c\delta p$ . Let  $A$  be the  $N_c \times N_c$  matrix obtained by deleting row  $N_c+1$  and column  $N_c+1$  from  $C$ . Let the  $N_c$ -row vector  $B$  be the first  $N_c$  entries of the last row of  $C$ . Then the IMPES reduction vector  $v$  (first  $N_c$  entries) is obtained from their transposes as

$$A'v = -B' \dots \dots \dots (6)$$

The reduction process gives three scalar transmissibilities  $\tau$  which are simply the dot or scalar products  $v \cdot T_{N_c+1}$ . A fourth dot product  $v \cdot R$  gives the scalar residual  $r$  and the IMPES pressure equation

$$c\delta p = \Delta(\tau\Delta\delta p) + r \dots \dots \dots (7)$$

Since  $v_{N_c+1} = 1$ , the dot products require only  $N_c$  multiplies. This reduction process gives a left-hand pressure coefficient  $c$  which reflects effects of changes in phase saturations, densities, and compositions.

An alternate IMPES reduction can be performed using Gaussian elimination to reduce the  $N_c+1 \times N_c+1$  main diagonal of the coefficient matrix,  $C$  and  $T_{jk}$  elements of  $T$ , to the identity matrix. This reduction facilitates the elimination of all terms in the constraint equations except pressure and wellbore pressure.

The IMPES procedure after calculation of  $E, C, T$ , and  $R$  is as follows. The linear solver solves equation 7 and the well

constraints for  $\delta p$  and the implicit wells'  $p_w$  values. The  $\delta p$  values are used to update interblock component flows to the new  $l+1$  iterate level. The  $C$  matrix coefficients are saved for well blocks. This allows solution for  $P_1, P_2, \dots, P_{N_c}$  for those blocks and updating of well rates. The new interblock flows and well rates are used as in the implicit case described above to obtain new phase compositions and saturations. The volume balance equation 5c is iterated out to tolerance and mass balance is exact.

In both cases, if any well  $p_w$  values are outside bottomhole pressure limits, (a) the Newton vector  $P$  is damped if necessary to avoid oscillating shutin, and (b) a subsequent Newton iteration is performed.

For the compositional case, the  $N_c$  phase equilibrium constraints are equality of liquid and vapor fugacities for each component. For the black oil case, the  $E$  matrix has only one nonzero column.

$$\delta y_1 = \frac{dY_1(p)}{dp} \delta p \dots \dots \dots (8)$$

$$\delta x_1 = \frac{dX_1(p)}{dp} \delta p \dots \dots \dots (9)$$

where the derivatives are obtained directly from the converted table.

In the compositional case, a Newton-Raphson flash calculation<sup>23</sup> is performed each Newton iteration for each three-phase block. It solves for  $N_c-1$  mole fractions and  $L$  or  $V$ . Phase disappearance is signalled by flash iterations outside the range  $0 < L < 1$ . For water-oil and gas-water blocks, Newton-Raphson  $p_{sat}$  calculations are performed and phase appearance is signalled by the sign of  $p-p_{sat}$ . In the event of flash failure, the model calculates  $p_{sat}$  to confirm the hydrocarbon single-phase state. In the event of  $p_{sat}$  failure, the mixture is flashed at a lower pressure and the resulting two phases are iteratively flashed back up toward block pressure  $p$ . The flash and/or  $p_{sat}$  calculations may fail due either to proximity to critical point or to passing out the right side of the pressure-composition phase envelope. The model avoids excessive flash and  $p_{sat}$  iterations and calculations by using stored historical data and by avoiding repeated attempts when composition has not changed sufficiently. The model senses when composition has moved to the right of the phase envelope and avoids the futile flash and  $p_{sat}$  calculations there. Typically a flash calculation requires only one to three Newton-Raphson iterations, fewer on the average in the implicit than in the IMPES case. Viscosities are obtained from the Lohrenz et al correlation<sup>24</sup>. Interfacial tension is obtained from the McLeod-Sugden correlation<sup>25</sup>.

In the black oil case a simple check of overall mole fraction  $z$ , against the converted table  $X_1(p)$  value detects phase appearance or disappearance. In both black oil and compositional cases, a block's phase configuration may change over the Newton iterations.

## Description of Well Calculations

Well calculations include the splitting or allocation of total well rate among the completed layers, the well constraint equation preserving target rate over the iteration, and special effects such as turbulence.

Holmes<sup>26</sup> described a splitting method which accounts for wellbore crossflow in implicit formulations. He assumed a fully-mixed wellbore and used three wellbore variables, two phase volume variables in addition to wellbore pressure. Modine et al<sup>27</sup> described an implicit splitting method which uses multi-node wellbore mass balances to eliminate the fully-mixed assumption in crossflow.

The splitting method used here is one Phillips Petroleum developed some years ago. It represents crossflow assuming a fully-mixed wellbore and uses the single wellbore pressure variable. It is simple and more efficient than the method of Modine et al. Wellbore pressure is

$$p_w(Z) = p_w + \gamma_{wb} (Z - Z^*) \dots \dots \dots (10)$$

where wellbore gradient  $\gamma_{wb}$  is approximated at the beginning of the time step and held fixed over the Newton iterations. We consider a production well completed in multiple layers of index  $k$ . Defining  $P_k$  as  $p_k - \gamma_{wb} (Z_k - Z^*)$ , the total rb/d  $Q_k$  and molar (moles/d)  $q_{ik}$  rates are:

for inflow layers ( $P_k > p_w$ )

$$Q_k = J_k \lambda_{wk} (P_k - p_w) \dots \dots \dots (11)$$

$$q_{ik} = J_k (\lambda_o \rho_o x_i + \lambda_g \rho_g y_i) (P_k - p_w) \dots \dots \dots (12)$$

$$q_{wk} = J_k \lambda_{wk} b_{wk} (P_k - p_w) \dots \dots \dots (13)$$

for outflow layers ( $P_k < p_w$ ),  $Q_k$  is the same as equation 11 and

$$q_{ik} = J_k f_i \lambda_{ik} (P_k - p_w) \dots \dots \dots (14)$$

$$q_{wk} = J_k f_w \lambda_{wk} (P_k - p_w) \dots \dots \dots (15)$$

where  $f_i = q_{i+} / Q_+$ ,  $f_w = q_{w+} / Q_+$  and the  $+$  denotes summation over all inflow layers. That is,  $q_{i+}$  is the summation of all inflow-layer  $q_{ik}$  molar rates,  $Q_+$  is the summation of all inflow-layer  $Q_k$  rb/d rates. This definition and use of  $f_i, f_w$

represents the fully-mixed wellbore assumption: the outflow stream is the same for all outflow layers and has the composition of the combined inflow streams. The interphase mass transfer and compressibility effects within the wellbore are neglected. All terms in the above equations are known or calculable from the single unknown  $p_w$ .

The well target rate  $q^*$  may be specified in any of nine different units, including stb/d oil, mcf/d gas, and total rb/d. For the simplest case of conventional black oil ( $r_s = 0$ , oil=component 1) and  $q^* =$  stb/d oil,

$$q^* = q_1 = q_{1+} + q_{1-} = q_{1+} \left(1 + \frac{Q}{Q_+}\right) \dots \dots \dots (16)$$

where  $q_{j+}$  and  $Q$  are the summations of  $q_{jk}$  and  $Q_k$  over all outflow layers. All terms on the right side of equation 16 are single-valued functions of  $p_w$ . Equation 16 is solved for  $p_w$  using Newton-Raphson iteration and  $q_{ik}^i$  are calculated from equations 12 and 14. The implicit molar rates required in the model are then

$$q_{ik} = q_{ik}^i + \delta q_{ik} = q_{ik}^i + \sum_{m=1}^N \frac{\partial q_{ik}}{\partial P_m} \delta P_m \dots \dots \dots (17)$$

The  $f_i, f_w$  values are iteratively lagged. All other terms in the  $q_{ik}$  expressions are differentiated with respect to  $p_w$  and all reservoir grid block variables  $y_i, x_i, S_w, S_o, S_g$ , and  $p$ .

The outflow curve gives  $p_w$  either as  $p_w = BHP$  or as a function of  $q_o$ , gas-oil ratio, and water cut given by a tubinghead pressure table. If the calculated  $p_w$  from equation 16 is above the outflow curve, the well is on target rate and a well constraint equation applies. If not, equation 16 and the outflow curve must be solved simultaneously for a  $p_w$  which is an intersection of the inflow (equation 16) and outflow curves. In this case there is no constraint equation if outflow  $p_w = BHP$  but there is in the tubinghead pressure table case<sup>28</sup>.

The constraint equation for the above black oil example is

$$\sum_{k=1}^2 \delta q_k = 0 \dots \dots \dots (18)$$

In black oil cases, the constraint equation exactly preserves target rate. The compositional case is more difficult. With  $q^* =$  stb/d oil specified, the constraint equation holding constant total moles/d,

$$\sum_{k=1}^2 \delta q_k = 0 \dots \dots \dots (19)$$

preserves surface oil rate only if the bottomhole inflow is an oil or gas phase of unchanging composition. The model uses a method<sup>29</sup> utilizing surface separation system overall K-values.

It gives a modified form of equation 18 which significantly reduces departure of the new rate from target value. This contributes to fewer Newton iterations, or better rates for the same number of iterations, in the compositional case.

It is well known that turbulent gas flow can affect gas injectivity in injection wells and producing rates and gas-oil ratio in production wells. Katz and Cornell<sup>30</sup> modified the Darcy flow equation to account for turbulence effects by introducing a turbulence factor  $\beta$  in the Forchheimer equation. The model uses a radially integrated form of that equation to relate  $p_w$  and gas rate<sup>28</sup>.

$$p_k - p_{wt} = \left[ \frac{1}{\lambda_g J \rho_g} q_g + \frac{41.125(10^{-16}) M \beta}{\rho_g r_w h^2} q_g^2 \right]_k \dots \dots \dots (20)$$

The term  $h^2$  is missing in reference 28, which describes in detail the modifications, for turbulence, in the layer gas rate calculation.

The turbulence factor  $\beta$  is presented graphically as a function of permeability and porosity by Katz et al<sup>31</sup>. The correlation of Firoozabadi<sup>32</sup> is used here,

$$\beta = f \frac{2.6(10^{10})}{(k_r k)^{1.2}} \dots \dots \dots (21)$$

where  $f$  has a default value of zero and may be entered as data for each perforated layer.

## Well Calculation Examples

Two examples are presented to illustrate the well calculation features in the model. First, an example which contains a considerable amount of wellbore crossflow is presented. Next, an example that includes the additional pressure drop which results from turbulent flow in the near wellbore region is discussed. All simulations reported in this paper were run on an IBM RS6000/590 using the XLF 3.1 compiler.

### Wellbore Crossflow Example

We have noted good accuracy of the wellbore crossflow method presented here in a number of  $x$ - $z$  cross-sectional problems. Three-dimensional dual-slice versions of such cross-sections can be run to give "exact" results<sup>28</sup>. The test problem presented here is a variant of the SPE2 10x15  $r$ - $z$  coning problem. The grid is a 10x15  $x$ - $z$  cross section of width 2500 feet, 2000 feet long with  $\Delta x$  equal to 200 feet. Data unchanged from SPE2 include layer properties, black oil PVT data, and relative permeability/capillary pressure data.

Depth to top center of grid block (1,1,1) is fixed at 9000 feet and the grid is rotated by a dip angle of 5.7 degrees, depths

increasing with increasing  $x$ . Zero vertical permeability is assigned between layers 5 and 6 and between layers 10 and 11, resulting in three isolated layer groups.

Initial conditions are capillary-gravitational equilibrium with a pressure of 3600 psia at a gas-oil contact depth equal to 9070 feet and with a water-oil contact depth of 9370 feet.

Three producers are specified in columns  $i=2$ ,  $i=5$ , and  $i=8$ . Well 4 is a 2000 stb/d water injector completed in layers 13-15 at column  $i=10$ . Producers 1-3 are completed in layers 11-13, 2-14, and 1-5, respectively. Their target production rates are 1000, 100, and 1000 stb/d oil, respectively, with minimum bhp of 1000 psia at their top perforations. Wellbore crossflow occurs in production Well 2. Layer productivity indices are calculated internally from the equation for a cross-section.<sup>33</sup>

$$J_k = \frac{.007084 kh}{\ln\left(\frac{w}{2\pi r_w}\right)} \text{ rb-cp/d-psi} \dots \dots \dots (22)$$

where  $kh$  is grid block md-ft.,  $w$  is the cross-section width, and  $r_w$  is equal to .5 feet.

Three five-year runs were made. Run 1 is the 2D  $x$ - $z$  cross-section with crossflow deactivated (production is only taken from layers where grid block pressure exceeds wellbore pressure and other layers are nonflowing). Run 2 is the same run with the wellbore crossflow calculation active. Run 3 uses a 3D 10x2x15 grid. The second slice  $j=2$  contains only Well 2 wellbore cells with their pore volumes equalling actual wellbore volume. The  $y$ -direction transmissibilities connecting these wellbore cells with their neighbors in slice  $j=1$  are equal to the Well 2 layer productivity indices  $J_k$  of Runs 1 and 2. Fractional flow ( $f = S$  for each phase) is used to represent the multiphase flow vertically within and out of the wellbore cells.

A comparison of results from these three runs is presented in Table 1 which includes original fluids in place for the three isolated regions in this problem as well as the remaining fluids in place at the end of five years. Average region pressures are also presented. Note the good agreement between the 2D run with crossflow and the "exact" 3D run. Significant differences are observed between the no crossflow and the crossflow run.

**Turbulent Gas Flow Example**

The effect of turbulent flow can also be expressed in terms of an apparent skin which varies with flow rate and is added to the laminar skin value.

$$s_{total} = s + Dq_g \dots \dots \dots (23)$$

The equation for calculating the non-Darcy flow coefficient,  $D$ , is comprised of the effects of three components for a perforated well: the compacted zone around perforation tunnels, the damaged zone due to drilling fluids and the reservoir rock properties<sup>34,35</sup>. These near wellbore effects can result in an equivalent  $\beta$  factor for poorly stimulated wells which is several orders of magnitude larger than values calculated for reservoir rock.

$$\beta_{effective} = \frac{hr_w\mu_g D}{2.226(10^{-15})k_r k G} \dots \dots \dots (24)$$

Values of  $f$  in equation 21 can be calculated as the ratio of  $\beta_{effective}$  divided by the  $\beta$  for reservoir rock.

The effects of turbulent flow are illustrated using SPE1 which has both a gas injection well and an oil producer. The maximum gas injection pressure was set equal to 7600 psia which is slightly higher than the value calculated versus time for this example when turbulent flow is negligible. A  $\beta$  multiply factor,  $f$ , of 50 for both the gas injector and oil producer was used to simulate near wellbore turbulent flow effects. This factor is conservative even for a well with six shots per foot and no near wellbore damage due to the perforation tunnels or drilling fluids. A comparison of the gas-oil ratio for this example with and without the effects of non-Darcy flow are presented in Figure 1. The lower gas-oil ratio shown for the run with turbulent flow calculations is a result of both reduced gas injection and gas production.

The reservoir rock effect alone ( $f = 1$ ) gives the following changes in SPE1 results at 3650 days: cumulative gas production is reduced from 338 to 304 Bscf and gas-oil ratio is reduced from 19697 to 17558 scf/stb.

**SPE Comparative Solutions**

Several SPE Comparative Solution Examples were run during the development of the model to test the accuracy of the results and the efficiency of the formulation. Three black oil problems, SPE1, Comparison of Solutions to a Three-Dimensional Black-Oil Reservoir Simulation Problem<sup>36</sup>, SPE2, A Three-Phase Coning Study<sup>37</sup> and SPE9, An Expanded Three-Dimensional Problem with a Geostatistical Distribution of Permeability<sup>38</sup>, were run as well as two compositional cases, SPE3, Gas Cycling of Retrograde Condensate Reservoirs<sup>39</sup>, and SPE5, Evaluation of Miscible Flood Simulators<sup>40</sup>. The number of time steps, Newton iterations and CPU time required for each run are presented in Table 2.

The SPE1, SPE3, and SPE5 problems have square  $xy$  grids and are symmetrical about the diagonal  $x=y$ . All runs reported here

used the full grids. These problems give identical results when run using the half symmetrical element, except that CPU times are reduced by a factor of about two.

Good agreement was obtained on results from these examples and those reported previously in the literature. The oil rate and gas-oil ratio for SPE1 and the cumulative oil and gas-oil ratio for SPE5, scenario one, are presented in Figures 1 and 2 for illustration. Results from SPE9 are included in the comparative solution project presented by Killough<sup>38</sup>.

## Field Examples

Three field examples are presented to demonstrate the utility of the model. The first example is a history match of the Ekofisk reservoir which includes both gas and water injection. The second example is a history match of gas cycling in the Chatom reservoir. The third example presents the simulation of slim tube and constant composition expansion experiments for the South Cowden CO<sub>2</sub> flood project.

### Ekofisk

The Ekofisk field, which is located in the Norwegian sector of the North Sea, was placed on production in July, 1971. Produced gas in excess of sales has been reinjected in the Crest of the field since 1975. Water injection was started in 1987 after a successful waterflood pilot was performed<sup>41</sup>. The waterflood was subsequently expanded<sup>42</sup> and currently water injection rates average 750,000 bbl/day.

A history match of the field from 1971-1994 was run. Reservoir and production(injection) data from Phillips reservoir simulation model<sup>43</sup> were used as input. A 13,728-block 44x26x12 grid with all cells active was used. The Phillips model extended beta PVT data were replaced by a three component description of Ekofisk<sup>28</sup>.

Field gas-oil ratio versus time for this run is shown in Figure 3 along with the results from Phillips model. Essentially identical results were obtained. The simulation was run using the IMPES formulation and took 265 time steps, 293 iterations, and 520 seconds of CPU time using conjugate gradient.

### Chatom

The Smackover Reservoir of the Chatom Field which is located in Washington County, Alabama is a retrograde gas condensate reservoir which contains approximately seventeen percent H<sub>2</sub>S. Liquid content of the gas at the dew point pressure of 3073 psig and reservoir temperature of 293 °F is 400 bbl/MMSCF.

Production from the field was started in 1974 and gas injection of residue gas was initiated in 1976.

A history match of this gas cycling project from 1974 to 1994 was conducted starting with data from a previous study<sup>44</sup>. A 4056-block 26x26x6 grid with 2214 cells active was used. The Soave-Redlich-Kwong equation of state with six components was used to match experimental phase behavior data which consisted of expansion and depletion experiments and swelling data. The composition of initial reservoir gas and injected gas are given in Table 1 of reference 44.

Results from this study are presented in Figure 4 which is a comparison of calculated and actual condensate rates versus time. This simulation took 702 time steps, 703 iterations and 241 CPU seconds using SOR.

### South Cowden

The South Cowden Unit, which is located in Ector County, Texas, was selected by the DOE as the site for the evaluation of an innovative CO<sub>2</sub> flood project. Advanced reservoir characterization technology will be used to describe the reservoir and to locate horizontal injection wells that will be drilled from a centralized facilities location<sup>45</sup>.

Preliminary simulation work on this project includes simulation of slim tube flooding experiments and the calculation of slim tube oil recovery versus pressure. The match of slim tube oil recovery measured at reservoir temperature of 98 °F and 1600 psia pressure using the Peng-Robinson equation of state is presented in Figure 5. The composition of reservoir fluid is presented in Table 3. The equation of state parameters were developed from matching differential liberation and constant composition expansion experiments on the original reservoir fluid and four constant composition expansion experiments of various mixtures of reservoir fluid and CO<sub>2</sub>, Figure 6. Calculated slim tube recovery versus pressure is shown in Figure 7 and varies from 40 percent at 600 psia to 95 percent at 1400 psia.

## Discussion

Several runs were made on SPE9 to investigate the level of time truncation error. Base runs using one and ten day time steps gave essentially identical results. Next, a run with sixteen time steps and fifty two iterations was made. Time truncation error in this run was apparent although not appreciably large. The last run was made with smaller maximum time step control and took thirty three time steps and fifty five Newton iterations, Table 2. The amount of time truncation error in this run is minimal.

## Conclusions

1. This paper describes a general three-phase, three-dimensional numerical simulation model. Black oil and fully compositional capabilities are included with IMPES and fully implicit formulations.
2. A relaxed volume concept is used in both IMPES and implicit formulations. It results in good volume balance, exact material balance and fewer Newton iterations.
3. A new implicit treatment of well rates provides increased stability for IMPES, approximates wellbore crossflow with good efficiency and relative simplicity, and includes near-well turbulent gas flow effects.
4. A normalization of relative permeability and capillary pressure is presented which allows these parameters to be calculated on a grid block basis.
5. Example problems are presented which illustrate the utility, efficiency, and robustness of the model formulations in black oil and compositional cases.

## Nomenclature

$b_w$	= water formation volume factor, stb/rb
$c_r$	= rock compressibility, 1/psi
$G$	= gas gravity, air equals one
$h$	= layer thickness, feet
$J_k$	= Layer $k$ productivity index, rb-cp/d-psi
$k$	= absolute permeability, md
$k_r$	= relative permeability, fraction
$k_{rgcw}$	= relative permeability to gas at connate water
$k_{rwswl}$	= relative permeability to water at $S_w = 1$
$M$	= gas molecular weight
$N$	= total number of variables, $2N_c + 4$
$N_c$	= number of hydrocarbon components
$N_w$	= number of active wells on target rates
$p$	= gas-phase pressure, psia
$p_b$	= base or reference pressure
$p_w$	= bottomhole wellbore pressure
$\bar{P}$	= $N_c + 1$ - vector of primary variables
$\bar{P}$	= $N$ - vector of total variables
$P_e$	= $N_c$ vector of eliminated variables
$P_c$	= capillary pressure, psi
$q_g$	= gas production rate, Mcf/d
$q_i$	= production rate of component $i$ , moles/d
$q_w$	= production rate of water, moles/d
$q^*$	= well target rate
$Q$	= production rate, total rb/d
$rb$	= reservoir barrel
$r_g$	= oil in gas phase, stb/scf
$r_w$	= wellbore radius, feet
$R_s$	= dissolved gas, scf/stb

$s$	= skin factor
$S$	= phase saturation, fraction
$S_{gc}$	= critical gas saturation
$S_{gr}$	= residual gas saturation
$S_{org}$	= residual oil saturation to gas
$S_{orw}$	= residual oil saturation to water
$S_{wc}$	= connate water saturation
$t$	= time, days
$\Delta t$	= time step, days
$T$	= transmissibility, rb-cp/d-psi
$v$	= IMPES reduction vector
$V$	= grid block volume, $\Delta x \Delta y \Delta z / 5.6146$ , rb
$x$	= mole fraction in liquid phase
$X_i, Y_i$	= mole fraction of oil in converted black oil table
$y$	= mole fraction in gas phase
$Z$	= subsea depth, ft
$Z^*$	= reference depth for flow bottom hole pressure

## Greek

$\alpha$	= $(1 - S_w - S_o - S_g)^i$
$\beta$	= turbulence factor, 1/ft.
$\bar{\delta}$	= $\bar{\delta}X = X_{n+1} - X_n$
$\delta$	= $\delta X = X^{i+1} - X^i$
$\gamma$	= gradient, psi/ft
$\lambda$	= mobility, $k_r/\mu$
$\mu$	= viscosity, cp
$\rho$	= phase density, moles/rb
$\phi$	= porosity, fraction
$\phi_b$	= grid block porosity at pressure $p_b$
$\tau$	= transmissibilities in the IMPES pressure equation

## Subscripts

$c$	= critical
$g$	= gas
$i$	= component number
$k$	= layer number
$l$	= iteration number (superscript)
$n$	= time step number
$o$	= oil
$w$	= water
$wb$	= wellbore

## Acknowledgements

The authors wish to express their appreciation to Phillips Petroleum Company for permission to publish this paper. Special thanks to Jim Sylte, Kim Juenger, and Ken Harpole for helping develop the field examples presented in the paper.



## References

1. Peng, D.Y. and Robinson, D.B.: "A Rigorous Method for Predicting the Critical Properties of Multicomponent Systems from an Equation of State," *AIChE J.* (1977) **23**, 137-144.
2. Soave, G.: "Equilibrium Constants for a Modified Redlich-Kwong Equation of State," *Chem. Eng. Sci.* (1972), **27**, 1197-1203.
3. Jhaveri, B.S., Youngren, G.K.: "Three-Parameter Modification of the Peng-Robinson Equation of State to Improve Volumetric Predictions," *SPE* (Aug. 1988) 1033-1040.
4. Peneloux, A., Rauzy, E., and Freze, R.: "A Consistent Correction for Redlich-Kwong-Soave Volumes," *Fluid Phase Equilibria* (1982) **8**, 7-23.
5. Sulak, R.M., Thomas, L.K., and Boade, R.R.: "3D Reservoir Simulation of Ekofisk Compaction Drive," *JPT* (Oct. 1991), 1272-1278.
6. Price, H.S. and Coats, K.H.: "Direct Methods in Reservoir Simulation," *SPEJ* (June 1974) 295-308; *Trans. AIME*, **257**.
7. Young, D.M.: "Iterative Methods for Solving Partial Differential Equations of the Elliptic Type," *Trans. Amer. Math. Soc.* (1954) Vol. 76, 92-111.
8. Thurnau, D.H.: "ESPIDO - What it Does and How it Works," Paper Number SSI 8603, SSI Technical Symposium, Denver, Co., 1986.
9. Wallis, J.: "Incomplete Gaussian Elimination as a Preconditioning for Generalized Conjugate Gradient Acceleration," paper SPE 12265 presented at the 1983 SPE Symposium on Reservoir Simulation, San Francisco, California, Nov. 15-18.
10. Watts, J.W.: "A Method for Improving Line Successive Overrelaxation in Anisotropic Problems - A Theoretical Analysis," *SPEJ* (April 1973) 105-118.
11. Bansal, P.P, Harper, J.L., McDonald, A.E., Moreland, E.E. and Odeh, A.S.: "A Strongly Coupled, Fully Implicit, Three-Dimensional, Three-Phase Reservoir Simulator," paper SPE 8329 presented at the SPE 54<sup>th</sup> Annual Technical Conference and Exhibition, Las Vegas, NV, Sept. 23-26, 1979.
12. Trimble, R.H. and McDonald, A.E.: "A Strongly Coupled, Fully Implicit, Three-Dimensional, Three-Phase, Well Coning Model," *SPEJ*, (Aug. 1981), 454-458.
13. Coats, K.H.: "An Equation of State Compositional Model," *SPEJ* (Oct. 1980) 363-376.
14. Young, L.C. and Stephenson, R.E.: "A Generalized Compositional Approach for Reservoir Simulation," *SPEJ* Oct. 1983, 727.
15. Acs, G., Doleschall, S. and Farkas, E.: "General Purpose Compositional Model," *SPEJ*, Aug. 1985, 543.
16. Watts, J.W.: "A Compositional Formulation of the Pressure and Saturation Equations," *SPE*, May 1986, 243.
17. Stone, H.L. and Garder, Jr., A.O.: "Analysis of Gas-Cap or Dissolved-Gas Drive Reservoirs," *SPEJ*, June 1961, 92.
18. Sheldon, J.W., Harris, C.D., and Bavly, D.: "A Method for Generalized Reservoir Behavior Simulation on Digital Computers," SPE 1521-G, 35th Annual SPE Fall Meeting, Denver, Colorado, Oct. 1960.
19. Wattenbarger, R.A.: "Convergence of the Implicit Pressure-Explicit Saturations Method," *JPT*, Nov. 1968, 1220.
20. Wattenbarger, R.A.: "Practical Aspects of Compositional Simulation," SPE 2800, Second Symposium on Numerical Simulation of Reservoir Performance, Dallas, Texas, Feb. 5-6, 1970.
21. Abel, W., Jackson, R.F., Wattenbarger, R.A.: "Simulation of a Partial Pressure Maintenance Gas Cycling Project with a Compositional Model, Carson Creek Field, Alberta," *JPT*, Jan. 1970, 285.
22. Coats, K.H.: "Reservoir Simulation: A General Model Formulation and Associated Physical/Numerical Sources of Instability", Boundary and Interior Layers - Computational and Asymptotic Methods, ed. by J.J.H. Miller, Boole Press, Dublin, Ireland (1980).
23. Fussell, L.T. and Fussell, D.D.: "An Iterative Technique for Compositional Reservoir Models," *SPEJ*, Aug. 1979, 211.
24. Lohrenz, J., Bray, B.G. and Clark, C.R.: "Calculating Viscosity of Reservoir Fluids from their Composition," *JPT*, Oct. 1964, 1171.
25. Reid, R.C. and Sherwood, T.K.: *The Properties of Gases and Liquids*, Third ed., McGraw-Hill Book Co. Inc., New York City, 1977.
26. Holmes, J.A.: "Enhancements to the Strongly Coupled, Fully Implicit Well Model: Wellbore Crossflow Modeling and Collective Well Control," paper SPE 12259 presented at the 1983 SPE Symposium on Reservoir Simulation, San Francisco, Nov. 15-18.
27. Modine, A.D., Coats, K.H., and M.W. Wells: "A Superposition Method for Representing Wellbore Crossflow in Reservoir Simulation", *SPE*, Aug. 1992.
28. Coats, K. H.: "Engineering and Simulation", Fourth International Forum on Reservoir Simulation, Salzburg, Austria, August 31 - September 4, 1992.
29. Coats, K.H.: "Implicit Compositional Simulation of Single Porosity and Dual Porosity Reservoirs", First

International Forum on Reservoir Simulation, Alpbach, Austria, September 12-16, 1988.

30. Cornell, D., and Katz, D.L.: "Flow of Gases Through Consolidated Porous Media," *Ind. Eng. Chem.*, **45**: 2145 (1953).

31. Katz, D.L., Cornell, D., Kobayashi, R., Poettman, F.H., Vary, J.A., Elenbaas, J.R., and Weinaug, C.F.: *Handbook of Natural Gas Engineering*, McGraw-Hill Book Company, Inc., New York City (1959).

32. Firoozabadi, A. and Katz, D.L., "An Analysis of High Velocity Gas Flow Through Porous Media," *JPT*, Feb. 1979, 211.

33. Coats, K.H. and Ramesh, A.B.: "Effects of Grid Type and Difference Scheme on Pattern Steamflood Simulation Results," *JPT*, May 86, 557.

34. McLeod, H.O., Jr: "The Effect of Perforating Conditions on Well Performance," *JPT* (Jan. 1983) 31-39.35

35. Thomas, L.K., Evans, C.E., Pierson, R.G., and Scott, S.L.: "Well Performance Model," *JPT*, (Feb. 1992), 220-229.

36. Odeh, A.S.: "Comparison of Solutions to a Three-Dimensional Black-Oil Reservoir Simulation Problem," *JPT*, Vol. 33, (Jan. 1981) 13-25.

37. Weinstein, H.G., Chappellear, J.E., and Nolen, J.S.: "Second Comparative Solution Project: A Three-Phase Coning Study," *JPT*, Vol. 38, (March 1986) 345-353.

38. Killough, J.H.: "Ninth SPE Comparative Solution Project: An Expanded Three-Dimensional Problem with a Geostatistical Distribution of Permeability," 1995 SPE Symposium on Reservoir Simulation, San Antonio, Tx, Feb. 12-15, 1995.

39. Kenyon, D.E., and Behie, G.A.: "Third SPE Comparative Solution Project: Gas Cycling of Retrograde Condensate Reservoirs," *JPT*, Vol. 39, (Aug. 1987) 981-998.

40. Killough, J., and Kossack, C.: "Fifth SPE Comparative Solution Project: Evaluation of Miscible Flood Simulators," paper SPE 16000 presented at the Ninth SPE Reservoir Simulation Symposium, San Antonio, Texas, February 1-4, 1987.

41. Thomas, L.K., Dixon, T.N., Evans, C.E., and Vienot, M.E.: "Ekofisk Waterflood Pilot," *JPT* (Feb. 1987), 221-232.

42. Hallenbeck, L.D., Sylte, J.E., Ebbs, D.J., and Thomas, L.K.: "Implementation of the Ekofisk Waterflood," *SPEFE*, (Sept. 91), 284-290.

43. Thomas, L.K., Dixon, T.N., and Pierson, R.G.: "Fractured Reservoir Simulation," *SPEJ* (Feb. 1983), 42-54.

44. Tompkins, M.W., Ebbs, D.J., Thomas, L.K., and Dixon, T.N.: "Chatom Gas Condensate Cycling Project," (Tech. Paper SPE 17353), *ATS*, (July 93), 152-160.

45. Hallenbeck, L.D., Harpole, K.J., Sistrunk, G.T., and Wier, D.R.: "Innovative Approach to CO<sub>2</sub> Project Development Holds Promise for Improving CO<sub>2</sub> Flood Economics in Smaller Fields Nearing Abandonment," paper SPE 28334 presented at the 69th Annual Technical Conference and Exhibition, New Orleans, LA, September 25-28, 1994.

46. Land, C.S.: "Calculation of Imbibition Relative Permeability for Two- and Three-Phase Flow from Rock Properties," *SPEJ*, (June 1968), 149.

47. Stone, H.L.: "Estimation of Three-Phase Relative Permeability and Residual Oil Data," *J. Cdn. Pet. Tech.* (Oct.-Dec. 1973) 53-61.

48. Thomas, L.K., and Coats, K.H.: "Stone's  $k_{rw}$  Methods and Modifications," SPE 25289, June, 1992.

**Appendix**

**Relative Permeability**

Relative permeability and capillary pressure curves are normalized using residual saturations, which can be entered on a grid block basis, and normalized saturation equations for the wetting and non-wetting phases. The normalized saturations range from zero to one for mobile phase saturations. Drainage  $P_{ow}$  and  $k_{rw}$  are normalized using  $S_w^*$ , where

$$S_w^* = \frac{S_w - S_{wc}}{1 - S_{wc}} \dots \dots \dots (A-1)$$

Imbibition  $P_{ow}$  and  $k_{row}$  are normalized using  $\bar{S}_w$ .

$$\bar{S}_w = \frac{S_w - S_{wc}}{1 - S_{wc} - S_{orw}} \dots \dots \dots (A-2)$$

The normalized saturations for  $k_{rg}$  and  $k_{rog}$  are  $S_g^*$  and  $\bar{S}_g$ , respectively.

$$S_g^* = \frac{S_g - S_{gc}}{1 - S_{wc} - S_{gc}} \dots \dots \dots (A-3)$$

$$\bar{S}_g = \frac{S_g}{1 - S_{wc} - S_{org}} \dots \dots \dots (A-4)$$

Relative permeability can be entered in tabular form or calculated from normalized saturations. If data are calculated they are then loaded into tables. Next the tabular data are normalized for use in the model.

The calculated  $k_r$  values are of Corey type, for example using an exponent of 2 gives

$$k_{rw} = k_{rwoil}(S_w^*)^2 \dots \dots \dots (A-5)$$

$$k_{rwo} = (1 - \bar{S}_w)^2 \dots \dots \dots (A-6)$$

and

$$k_{rg} = k_{rgcu}(S_g^*)^2 \dots \dots \dots (A-7)$$

$$k_{rog} = (1 - \bar{S}_g)^2 \dots \dots \dots (A-8)$$

Hysteresis in  $k_{rg}$  is calculated using a modification of Land's equation<sup>28,46</sup>. Residual gas saturation,  $S_{gr}$ , is a function of historical maximum gas saturation. Three phase oil relative permeability is calculated using Stone's first method<sup>47</sup> with variable  $S_{or}$ <sup>48</sup> or optionally using Stone's second method.

**SI Metric Conversion Factors**

bbbl	x 1.589 873	E-01	=	m <sup>3</sup>
cp	x 1.0*	E-03	=	Pa·s
cu ft	x 2.831 685	E-02	=	m <sup>3</sup>
° F	(°F - 32)/1.8		=	° C
ft	x 3.048*	E-01	=	m
psi, psia	x 6.894 757	E+00	=	kPa
psi <sup>-1</sup>	x 1.450 377	E-01	=	kPa <sup>-1</sup>

\*Conversion factor is exact

**Table 1**  
**2-D Cross-section with Cross Flow**

Region	Fluids in Place			Average Pressure psia	Case, Time
	Water MSTB	Oil MSTB	Gas MMSCF		
1	2107	5963	9319	3620	Initial Conditions
2	2034	4950	6882	3646	
3	18572	5742	7983	3703	
1	2198	4787	3600	1245	2D with Crossflow 5 Years
2	2022	4063	3082	1413	
3	19205	4525	3218	1533	
1	2221	4787	3522	1221	3D "Exact" 5 Years
2	2031	4067	3053	1402	
3	19179	4543	3228	1530	
1	2095	4708	2943	1002	2D no Crossflow 5 Years
2	2033	4862	6761	3497	
3	19557	4292	2973	1519	

**Table 2**  
**SPE Comparative Solution Projects**

Project	$N_c$ - Grid	Formulation-Soln Algorithm	Number Time Steps	Newton Iterations	CPU Time, sec
SPE1	2 - 10x10x3	Fully Implicit-CG	24	63	5.2
		IMPES-D4	254	256	7.0
SPE2	2 - 10x1x15	Fully Implicit-D4	15	30	2.2*
SPE3	9 - 9x9x4	IMPES-D4	113	114	21.5
		Fully Implicit-CG	32	44	30.8
SPE5	6 - 7x7x3	Scenario 1			
		IMPES-D4	468	471	23.6
		FI-CG	46	174	31.6
		Scenario 2			
		IMPES-D4	670	672	21.9
		FI-CG	58	248	37.5
		Scenario 3			
		IMPES-D4	527	531	24.6
		FI-CG	47	190	36.9
SPE9	2 - 24x25x15	Fully Implicit-CG	33	55	101.8

\*CPU time for this case was .9 sec. with 1.3 sec. for data input, initialization, and error checking. All CPU times reported in this table include similar overhead.

**Table 3**  
**South Cowden Reservoir Fluid Composition**

Normalized Feed Mole Fractions

Component	Number	
N <sub>2</sub>	1	0.0047
CO <sub>2</sub>	2	0.0066
H <sub>2</sub> S	3	0.0209
C <sub>1</sub>	4	0.1150
C <sub>2</sub>	5	0.0575
C <sub>3</sub>	6	0.0704
IC <sub>4</sub>	7	0.0156
C <sub>4</sub>	8	0.0447
IC <sub>5</sub>	9	0.0249
C <sub>5</sub>	10	0.0239
C <sub>6</sub>	11	0.0699
C <sub>7+</sub>	12	0.5459
	Sum:	1.0000
C <sub>7+</sub> Molecular Weight		228.00
C <sub>7+</sub> Specific Gravity		0.8784
Reservoir Temperature		98 °F

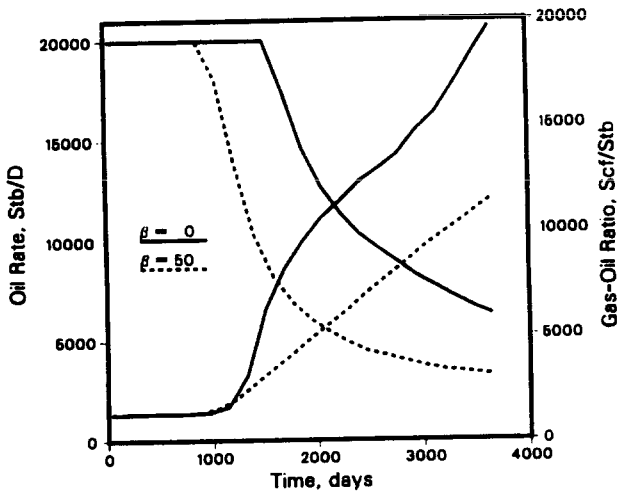


Fig. 1 - SPE1 Oil Rate and Gas-Oil Ratio vs. Time.

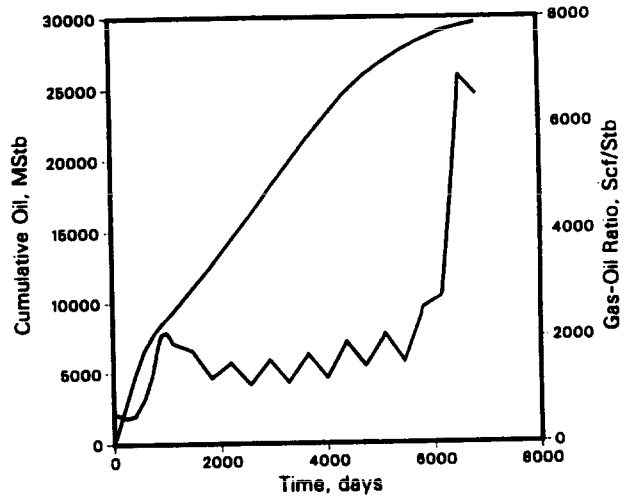


Fig. 2 - SPE5 Cumulative Oil and Gas-Oil Ratio vs. Time.

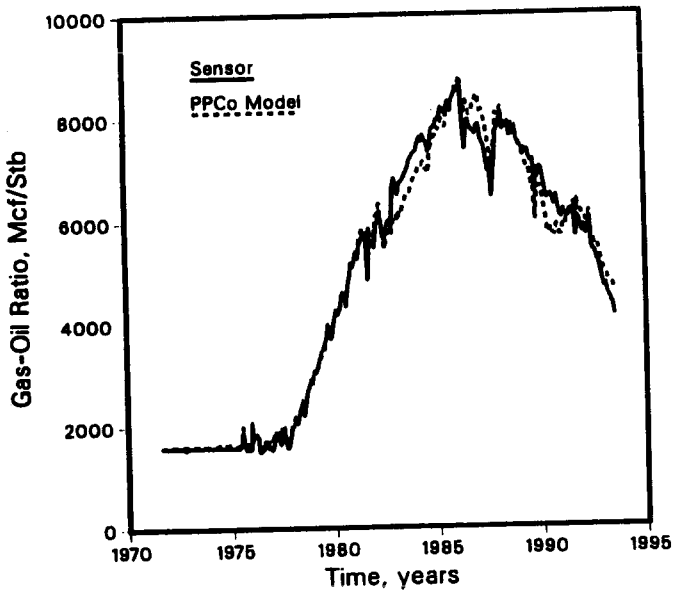


Fig. 3 - Ekofisk Field - Gas-Oil Ratio Match

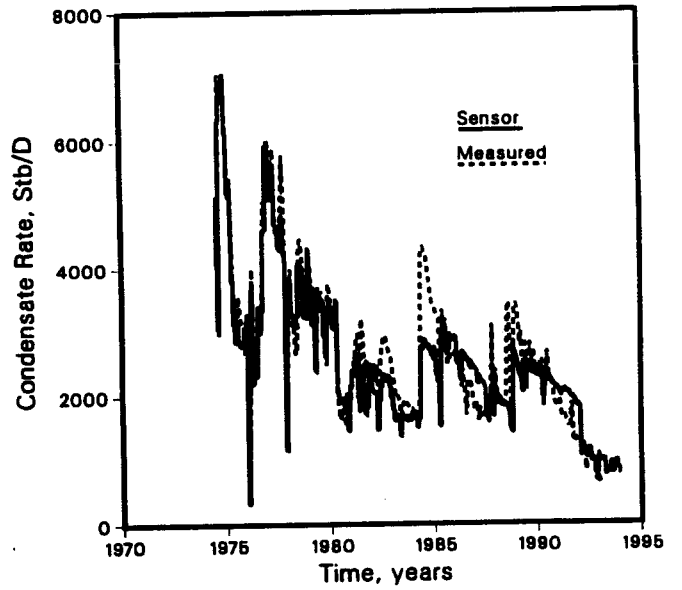


Fig. 4 - Chatom Condensate Rate vs. Time

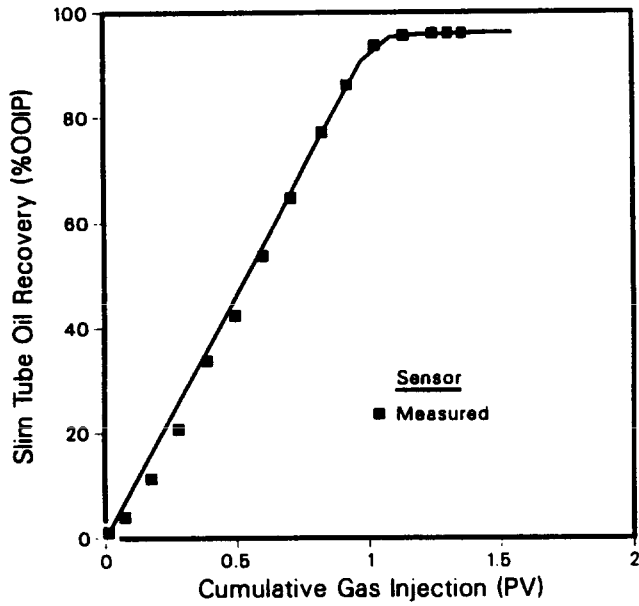


Fig. 5 - South Cowden Slim Tube Simulation @ 1600 psi

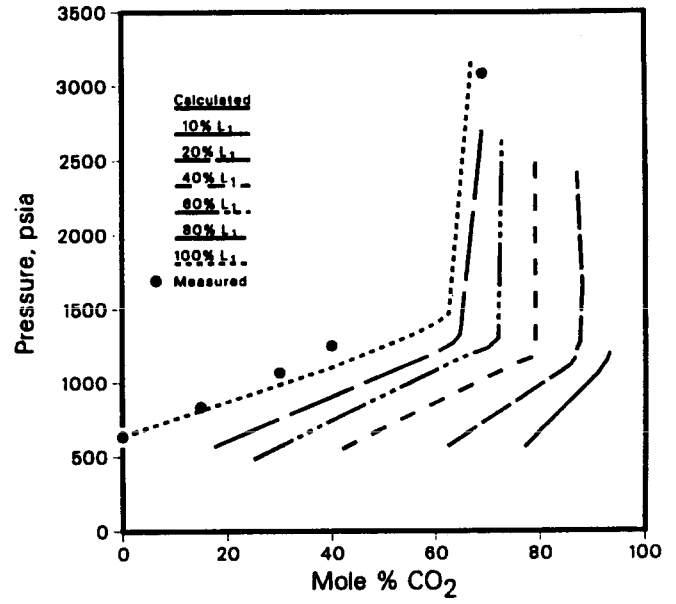


Fig. 6 - South Cowden Pressure vs. Composition Diagram

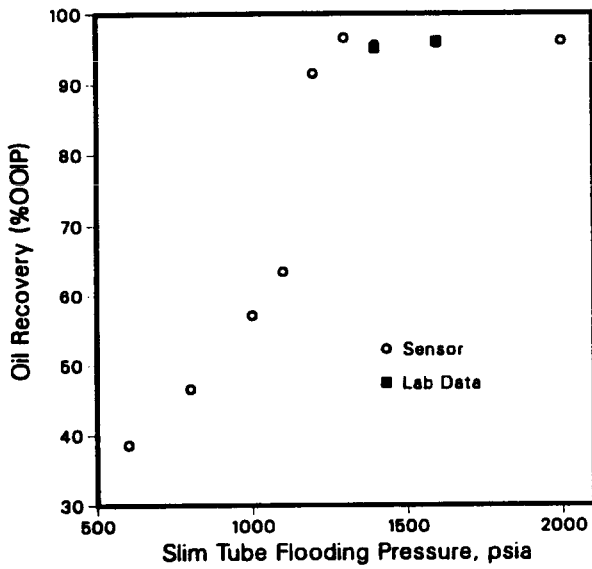


Fig. 7 - South Cowden Slim Tube Recoveries @ 1.2 PV CO<sub>2</sub> Injected